2012 IEEE/RSJ International Conference on
Intelligent Robots and Systems
October 7-12, 2012. Vilamoura, Algarve, Portugal

Path Planning based on Reaction-Diffusion Process

Alejandro Vázquez-Otero[1], Jan Faigl[2], Alberto P. Muñuzuri[1]

Abstract— **In this paper, we present a novel path planning algorithm based on properties that reaction-diffusion (RD) models exhibit by the underlying non-linear dynamics of the considered system. In particular herein considered a two-variable RD model provides advantages of natural parallelism, noise resistance, and especially the non-annihilating feature that traveling fronts separating two stable states exhibit upon a collision. Based on this, we developed a path planning algorithm that provides paths with lengths competitive to standard path planning approaches. Moreover, the results presented indicates the paths are smoother and also within a safe distance from obstacles; thus, the found paths combine advantages of two fundamental approaches, namely the DT algorithm and Voronoi diagram.**

I. Introduction

This paper is concerned with an autowaves based path planning algorithm for navigating a mobile robot. The type of dynamics described by reaction-diffusion (RD) models occurs in many systems ranging from physical, chemical, or biological, e.g., excitation waves in the heart muscle. An RD model describes evolution of a vector of at least two components, where the information exchange takes place via a diffusive process. Thus, the evolution is expressed as spatio-temporal concentration profiles that can exhibit complex patterns as self-sustained structures [1].

RD systems can be numerically reproduced as a network of coupled cells with short-range coupling, which greatly simplifies its codification and enables a direct hardware implementation by means of standard technologies (GPU, FPGA, VLSI). Even more, combination of the intrinsic massive parallelism of the model propagation and the short-range diffusive coupling between cells results in a fault tolerance that can be interpreted as noise resistance (isolated damage cells do not influence the overall behaviour), exposing the robustness of natural phenomena. These interesting properties have already been explored in the context of computational analysis as a set of image processing operations [2], [3], [4], [5], [6]. For the calculation of the shortest time to reach a destination point [7], and more recently, the shortest path between two points [8].

This work was supported by the Ministerio de Educación y Ciencia and Xunta de Galicia under Research Grants No. FIS2010-21023 and No. PGIDIT07PXIB-206077PR. The work of Jan Faigl has been supported by the Technology Agency of the Czech Republic under Project No. TE01020197.

[1]A. Vázquez-Otero and A. P. Muñuzuri are with the Group of Non-Linear Physics, University of Santiago de Compostela, 15782 Santiago de Compostela. Spain alejandro.vazquez@usc.es, uscfmapm@cesga.es

[2]J. Faigl is with the dept. of Cybernetics, Faculty of Electrical Engineering, Czech Technical University in Prague, Technická 2, 166 27 Prague, Czech Republic xfaigl@labe.felk.cvut.cz

The use of RD systems for path planning (or a mobile robot navigation task) is not a new idea and several approaches have been already proposed following both perspectives: experimental and strictly computational. The pioneering work has been introduced by Adamatzky [9], [10] and Trevai et al. [11], [12] whom respectively demonstrated feasibility of both approaches.

Although several consecutive approaches using the underlying RD process have been proposed, e.g., [13], [14], [15], [16], [17], the presented approach differs conceptually, as the change of phase method in combination with new properties recently achieved by the authors; hence it constitutes a completely new approach for solving optimization problems using an RD system. Moreover, none of the previous approaches (to the best of our knowledge) provide a comparison with approaches well established in robotics. Therefore, in this paper, we compare the proposed novel RD path planning algorithm with two standard approaches for planning on a grid representation of the robot working environment. The selected approaches are the Distance Transform algorithm [18] and extended Voronoi graph (EVG) [19].

The considered non-annihilating feature regarding front-wave collision in a particular bistable configuration of the RD system has been effectively used recently [8], [20]. This small step of generating computational autowaves that do not annihilate upon a collision contains a fundamental consequences from the information processing point of view, as the position of collisions now remains in the natural evolution of the model. All previous attempts to develop algorithms using autowaves commonly rely on iterative processes, forcing to restart the computations at the positions where annihilation took place. Positions that also had to be recorded onto a memory system each time the computations were restarted. Regarding this, the approach presented in this paper can be considered as a use case of the RD-system's computational model applied in mobile robotics. The model used forms a solid base of a unified way based on biological processes to solve additional navigational problems. Thus, the approach represents a new class of path planning algorithms based on different principles than the well-establish planning methods already used in robotics.

The paper is organized as follows. The next section provides fundamentals of the autowaves approach. In Section III, the proposed path planning algorithm based on the RD model is presented and particular implementation issues are described. A comparison of the algorithm with standard approaches is presented in Section IV together with an example of the experimental deployment demonstrating real applicability of the proposed approach. Finally, Section V is

dedicated to concluding remarks.

II. Basic Autowaves Background

A detailed description of RD system dynamics in which the autowaves phenomena occur is out of the scope of this paper, therefore, here we present an overview of the autowaves, the considered RD model, and a straight-ahead description toward the main principles used in the proposed path planning algorithm.

Autowaves represent, by definition, a particular class of nonlinear waves that propagate through an active media at the expense of the energy stored in the medium and are manifestations of a strongly nonlinear active media [21].

Reaction-diffusion models are a type of dynamical systems that are able to reproduce autowaves. The simplest way to write an RD equation capable of generating autowaves is by the system of two equations

$$\begin{array}{rcl} \dot{u} & = & f(u,v) + D_u \triangle u \\ \dot{v} & = & g(u,v) + D_v \triangle v \end{array} . \tag{1}$$

This system describes the evolution of the state variables $u = u(\vec{x}, t)$ and $v = v(\vec{x}, t)$, where the so-called activator u influences positively on the formation of both u and v, whereas the so-called inhibitor v tends to decrease the concentration of v, by means of the functions $f(u,v)$ and $g(u,v)$, that takes into account biochemical aspects of the system and represents the local rate at which the substances (or morfogens) (u,v) are converted into each other at any time. The laplacian terms $\triangle u$ and $\triangle v$ representing the diffusive coupling between cells stand for the spreading of the substances out in the space.

Although the non-linear properties are generic, here, the two-variables FitzHugh-Nagumo (FHN) model [22] is used for a practical realization:

$$\begin{array}{rcl} \dot{u} & = & \varepsilon\left(u - u^3 - v + \phi\right) + D_u \triangle u \\ \dot{v} & = & (u - \alpha v + \beta) + D_v \triangle u \end{array} , \tag{2}$$

where α, β, ϵ, and ϕ are parameters of the model.

The general dynamics of the RD system is determined by the associated *nullcline configurations* and those in turn are the geometric shape (see Fig. 1) for which $\dot{u} = 0$ (and $\dot{v} = 0$) in the absence of diffusion:

$$\begin{array}{rcl} \varepsilon\left(u - u^3 - v + \phi\right) & = & 0 \\ (u - \alpha v + \beta) & = & 0 \end{array} . \tag{3}$$

The *fixed points* of the system are the ones represented by the nullclines intersection, and basically can be classified in stable and unstable states, leading to stable steady states (SS) or conversely to unstable steady states (US). Concentration levels of the state variables (u,v) evolve naturally toward the concentration levels determined by SS. For the purpose of this work we are concerned with the nullcline configuration depicted in Fig. 1a leading to the so called *bistable regime* in which the model presents two SS and one US (green and red discs, respectively). It basically means that the system (i.e., the concentration levels of (u,v) for each grid-cell) tends to remain in any of this two SS, being feasible that some portions of the system be in one, while the remaining parts be in the other. Consequently, an interesting property of the bistable regime lies in the possibility to modulate the relative stability of both SS. Allowing to differentiate between SS^+ and SS^- that clearly represent the more and less SS respectively. Moreover, the relative stability of both SS can be trivially related with the area under the curve, which is reproduced in Fig. 1c and Fig. 1b. Thus, the *relative stability* of the system can be modulated through the nullcline configuration.

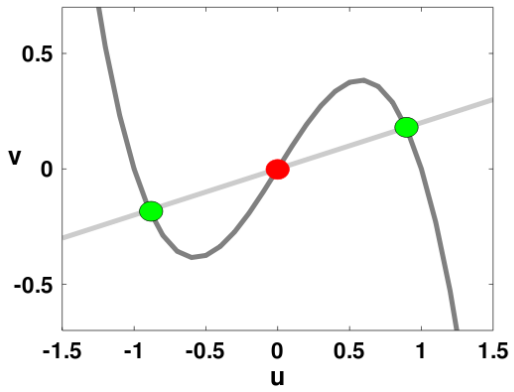

(a) General nullcline configuration corresponding to a bistable system. Green discs shows the stable states, while the red disc shows the unstable one.

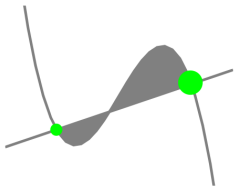

(b) Rightmost SS corresponds to SS^+ during propagation phase.

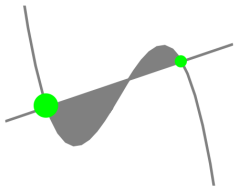

(c) Leftmost SS corresponds to SS^+ during contraction phase.

Fig. 1. Nullcline configuration, the green disks represent SS and the red represent US.

Finally, as the system evolves toward the concentration level of SS^+, a default configuration in SS^- causes the system to move to SS^+ if a small perturbation is introduced. Under these circumstances the mobile frontier that separates both SS and drives the shift can be considered as a *traveling frontwave*. Thereby, only this type of autowaves is used in this work.

A. RD-System Dynamics Involved in Path Planning

The aforementioned bistable regime of the RD model in a combination with the non-annihilation feature provides a solid framework for developing a path planning algorithm. Therefore, a brief description of the RD dynamics involved is a desirable introduction to the proposed planning approach.

A visualization of the model state using a basic integration sequence is depicted in Fig. 2. The sequence consists of two phases: *propagation* and *contraction*. Each phase is governed by a different nullcline configuration, so that in the *propagation* phase the rightmost SS is more stable: $(SS^+)_{launch}$, and conversely in the *contraction* phase the leftmost SS is more stable: $(SS^+)_{contract}$.

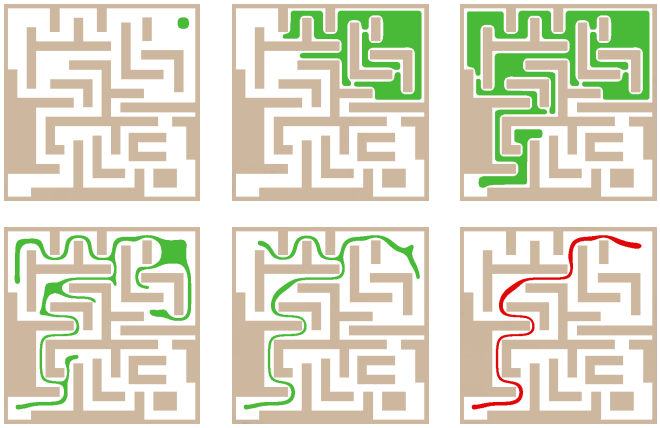

Fig. 2. An example of the system evolution; *upper*: propagation phase; *bottom*: contraction phase. The freespace is in white and obstacles in dark, the green denotes parts of the system that are in the SS^+ states, and the final solution is in red.

Propagation phase: following the series of pictures in Fig. 2 the whole system (let say background) is set in $(SS^-)_{launch}$ at the beginning of the process, except a small region representing the starting point that is set in $(SS^+)_{launch}$. This initial small region spreads itself in parallel throughout the labyrinth covering all possible paths. Along this propagation, as the traveling front leading the shift is sometimes split because of obstacles. It also often results in two fronts collision at intersections. But here the *non-annihilation* property (exhibit due to the specific model-configuration used in this work), plays a key role: one front branch usually remains stationary at this point while the other continues propagating and leading the shift (the other possibility is that both fronts remain static at this point). In any case, annihilation of frontwaves under collision never takes place.

Contraction phase: When the autowave reaches the goal, the *contraction* phase is activated. The nullcline configuration now corresponds to that one in Fig. 1c and the system starts to move towards $(SS^+)_{contract}$. The sequence of pictures in Fig. 2 (bottom row) shows how all regions resting in $(SS^-)_{contract}$ start shrinking at the expenses of $(SS^+)_{contract}$ that grows up.

Finally, a simple technique to extract the shortest path connecting the initial position with the goal position within the computational grid is used. While the relative stability switch leading to the *contraction* phase is activated (right at the end of the *propagation* phase), both regions representing the start and goal positions inside the domain $(SS^-)_{contract}$ are forced to maintain such a level of concentration, in spite of the system tendency toward $(SS^+)_{contract}$.

Consequently (as it can be observed in Fig. 2) all branches of the domain $(SS^-)_{contract}$ start shrinking until they completely disappear, remaining only a single path that links the two forced points, i.e., the shortest path connecting the start and goal locations, see the right bottom picture in Fig. 2.

B. A Summary of the Computational Model

The computational system consists of a grid of diffusion-coupled cells, and the evolution of each cell is described by the FHN model set in a bistable regime. The employed discretization is the common finite difference method on a Cartesian grid with Dirichlet boundary conditions: a simple forward in time centered in space (FTCS).

On the other hand, since the FHN-RD model is derived from a biochemical one, the information that provides is the concentration level of u and v. Thus, introducing information into the system is basically constraining the concentration levels in adequate places to some specific values. This process is usually known as *external forcing*, and here, it is undertaken through the local modification of nullclines configuration for the cells of interest.

Regarding practical usage of the RD dynamics in solving the path planning problem, the grid based representation of the robot working environment is considered. A grid map is used to force the concentration levels in the computational grid in order to represent obstacles, the start and the goal locations. The computational model needs a particular size of the computational grid in order to exhibit the full behaviour of the RD system. Therefore, it is necessary to abide these requirements together with particular physical dimensions of the robot and its working environment. Based on the experimental and theoretical analyses it is necessary to have at least 24 grid cells for propagating the frontwaves (e.g., through a narrow passage)[1]. Having a robot with a shape that can be bounded by a disk with a diameter d, then the dimensions of the computational grid should be at least $24w/d \times 24h/d$ including the map borders, where w and h represent real dimensions of the environment.

III. Path Planning Based on Autowaves

The aforementioned computational model of the RD system provides the main principle for the proposed path planning algorithm. Although the core of the algorithm is an integration step of the FHN model, it has to be complemented by additional functions to be usable for finding a path in a map of the robot working environment. The algorithm is a two phases procedure. In the first phase, a frontwave is propagated through the environment model until the goal location is reached. An exhibition of this phase is similar to the wavefront algorithm well-known in robotics; however, in this case the internal principles are based on the underlying RD model. The second phase is a contraction in which a path is formed. The path is represented by different values of the concentration level, therefore it has to be extracted from the computational grid. The path planning algorithm can be summarized as follows.

- Let $\mathcal{G}$ be the computational grid, $\mathcal{W}$ be a grid map of the robot working environment, and g_s and g_e be initial and desired positions of the robot within $\mathcal{W}$, respectively. The grid consists of several matrices representing particular variables of the model (2). A particular robot position within the grid addresses a particular cell in

[1]Due to a page limited only the result of the analyses are presented here. Besides, detailed description of the analyses is also out of the scope of the paper, and it is going to be published in a dedicated paper.

a matrix, e.g., $\mathcal{G}_u(g_s)$ represents the value of u at the position g_s.

- **Propagation Phase**
  1) Initialization - set model parameters (forcing):
     - Initialize u and v, e.g., $\mathcal{G}_u$ = -0.9, $\mathcal{G}_v$ = -0.22.
     - Set border to avoid the propagation out of the computational grid.
     - Forcing robot position.
  2) Perform one integration step according to (2).
  3) Termination Condition - if the frontwave reaches g_e go to Step 4, otherwise repeat integration Step 2.
- **Contraction Phase**
  4) Initialize - set model parameters (forcing).
  5) Perform one integration step according to (2).
  6) Termination Condition - $|\dot{u}| < \epsilon$, where $\epsilon > 0$ - if a static situation has been reached continue with the path extraction, otherwise go to Step 5.
- **Path Extraction**

Each phase of the algorithm is basically an integration loop that is terminated once a static situation is reached. However, the termination condition can be a bit tricky because of underlying chemical process, which can have very long time constants. Therefore, the integration is terminated once the frontwave reaches the goal position in the propagation phase, i.e., $\mathcal{G}_u(g_e) > 0$. In the propagation phase, the activity (changes of the concentration levels) is mainly at the front wave. Contrary to the contraction phase, in which the concentration levels are changed more dramatically due to a longer band of reacting border of parts with different concentrations. After the initial fast contraction, the process becomes a bit slower. In this case, the integration can be terminated if changes in the concentration level of u are small, e.g., using T steps period $|u(t)-u(t+T)| \leq 0.001$. The used parameters of the underlying FHN model are: α=5.0, ϵ=10.0, D_u=0.1, D_v=1.5, and β=-0.2 in the propagation phase and β=0.1 in the contraction phase.

Path Extraction – Once the contraction phase is terminated, the solution found is represented by the grid cells with $u > 0$. A path in a form of a sequence of desired robot positions can be then determined using a searching algorithm considering these cells. The cells form a corridor in the grid, see Fig. 2 for an example. Voronoi diagram of the corridor is constructed and the final path is found using Dijkstra's algorithm.

Implementation Notes – The computational complexity of the underlying process depends on the discretization of the laplacian, which can by bounded by $O(1)$ for computing a single cell; however, the whole integration step depends on the grid size. Hence, the integration can be computationally demanding, especially for a large sized grid. On the other hand, the integration can be easily parallelized, e.g., using the OpenMP technology. Moreover, we addressed the high computational requirements by monitoring active cells (cells where the integration takes place, which basically corresponds to the wavefront) since after reaching the concentration level of the corresponding SS they remain in a static situation. A combination of the parallelization with the monitoring results the computational burden is significantly reduced (up to three orders of magnitude). In terms of the real required computational time a path through the whole environment is found in tens of minutes using a 1000×1000 grid and four cores of CPU running at 3.2 GHz. Without these optimizations the same computation needs a couple of hours.

IV. Comparison with Standard Approaches

The proposed path planning algorithm has been experimentally verified in several simulations regarding its applicability in robotic problems. In this section, the performance of the proposed autowaves based planning approach is compared with two state-of-the-art (grid based) approaches. The first approach is the Distance Transform (DT) algorithm [18]. The second approach is based on the Voronoi diagram computed on a grid using the approach [19]. The diagram is then converted into a graph in which final path is found by Dijkstra's algorithm. A disc robot with radius ρ is assumed, and therefore, obstacles are enlarged appropriately using the discrete version of the Minkowski Sum to find a path within a safe distance from the obstacles.

The quality metrics are the length of the path found l, and the minimal, maximal and average distances from each path's point (grid cell) to the closest obstacle denoted as d_{min}, d_{max} and d_{avg}, respectively. The path length and distances are computed as the Euclidean distances between the cells' centers.

Although the approach has been tested within several environments, herein presented results have been computed using the *var_density* environment because of page limit. The environment is relatively complex as it contains many narrow passages; thus, it provides the opportunity to find different paths according to the robot's dimensions. Three problems are considered in this environment that are denoted as *p1*, *p2* and *p3*. In addition, three radiuses of the disc representing the robot has been considered $\rho \in \{0.3, 0.2, 0.15\}$ (in meters), which determine an appropriate size of the computational grid. For each problem all values of ρ have been considered and the paths have been found by the all evaluated methods. Thus, the total number of the evaluated problems is nine and the total number of found paths is 27.

(a) DT-algorithm (b) Voronoi diagram (c) Autowaves

Fig. 3. Found paths for the problem *var-density*-p1, robot with $\rho = 0.30$ m and the size of the computational grid 2350×2350.

Results are presented in Table I and selected found paths are visualized in Fig. 3, Fig. 4, and Fig. 5. Regarding the

TABLE I

PATH LENGTH AND QUALITY WITHIN THE *var_density* ENVIRONMENT

Problem	Grid	ρ [m]	Distance Transform				Voronoi Diagram				Autowaves			
			L	d_{min}	d_{max}	d_{avg}	L	d_{min}	d_{max}	d_{avg}	L	d_{min}	d_{max}	d_{avg}
p1	2370×2370	0.30	42.2	0.30	1.49	0.55	48.9	0.32	1.85	0.92	47.1	0.30	1.47	0.89
p1	2220×2220	0.20	37.2	0.20	1.49	0.48	44.3	0.24	1.84	0.88	41.7	0.22	1.46	0.82
p1	1270×1270	0.15	28.5	0.15	1.65	0.58	35.4	0.17	1.84	0.99	31.0	0.16	1.56	0.79
p2	2370×2370	0.30	42.7	0.30	1.72	0.60	48.4	0.32	1.85	0.92	46.1	0.30	1.75	0.92
p2	2220×2220	0.20	37.9	0.20	1.67	0.53	43.7	0.24	1.84	0.88	41.1	0.22	1.73	0.87
p2	1270×1270	0.15	23.4	0.15	1.65	0.44	28.8	0.15	1.63	0.81	25.7	0.16	1.56	0.63
p3	2370×2370	0.30	24.5	0.30	1.14	0.52	27.2	0.32	1.52	0.76	25.0	0.30	1.29	0.67
p3	2220×2220	0.20	20.2	0.20	1.27	0.40	22.6	0.24	1.51	0.66	21.8	0.22	1.35	0.72
p3	1270×1270	0.15	20.1	0.15	1.21	0.50	22.5	0.24	1.51	0.66	21.3	0.20	1.22	0.66

(a) DT-algorithm (b) Voronoi diagram (c) Autowaves

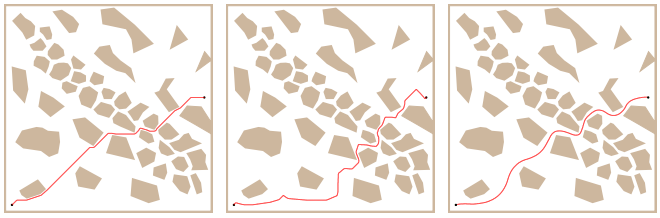

(d) DT-algorithm (e) Voronoi diagram (f) Autowaves

Fig. 4. Found paths for the problem *var-density*-p2, the robot size ρ and two grid sizes; *top*: $\rho = 0.20$ m and the grid 2200×2200; *bottom*: $\rho = 0.15$ m and the grid size 1250×1250.

(a) DT-algorithm (b) Voronoi diagram (c) Autowaves

Fig. 5. Found paths for the problem *var-density*-p3, robot size $\rho = 0.15$ m and the grid size 1250×1250.

quality metrics the proposed path planning approach provides competitive solutions to the standard algorithms. It provides safer paths than the DT (regarding d_{avg}) and also they are shorter than Voronoi diagram paths. In addition, the main benefit of the autowaves paths is evident from the figures. The paths are smooth, while they are not significantly longer than the shortest paths found by the DT.

A. Real Deployment of the Proposed Method

A real applicability of the developed path planning method has been verified using a map of the environment built automatically by a mobile robot.

The considered robot G^{2}Bot (developed at the dept. of Cybernetics, FEE, CTU in Prague) [23] has been equipped

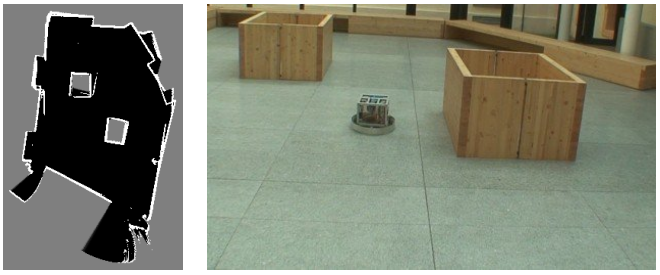

(a) Occupancy grid (b) G^{2}Bot in the experiment

Fig. 6. A raw occupancy grid acquired using SICK laser range finder and G^{2}Bot.

(a) initialization (b) propagation (c) contraction (d) a path found

Fig. 7. Steps of the underlying RD-system evolution using the built map from the occupancy grid.

with the SICK LMS200 laser range finder, and the map has been built using the probabilistic occupancy grid, see Fig. 6. Then, the grid has been used for forcing the computational grid of the RD model and path has been found, see a sequence depicted in Fig. 7. The main advantages of the proposed path planning approach is its ability to deal with noisy data that do not influence smoothness of the final path as can be seen in Fig. 7d.

B. Discussion

The results indicate that the proposed path planning provides competitive paths to the standard approaches. Moreover, the paths found are shorter than paths provided using the Voronoi diagram and they are also safer than paths found by the DT regarding distance from the robot towards the obstacles along the path. In addition, paths provided by the proposed planner are smoother, which also holds for maps built from the real sensors, which suffers from sensor noise.

On the other hand, the underlying RD model makes the implementation further computationally demanding, in comparison with the tested standard approaches. However,

the model is strongly parallelizable and with a combination of the current progress in massive parallel processing, e.g., GPU and related technologies (or eventually implementation via VLSI or similar architecture), it can be expected this will not be a significant issue in the future.

The observed smoothness of the found paths is an interesting feature of the proposed approach as it does not explicitly consider a robot dynamic. The smoothness comes from the biochemical underlying processes. Moreover, during the experimenting we have found out that the model parameters affect the dynamic of the propagation (i.e., the frontwave propagation in a narrow passage is slower). These findings make us a bit optimistic for a further research about including a robot dynamic into the proposed approach.

V. Conclusion

In the presented study, a novel path planning algorithm based on the general dynamics provided by the FitzHugh-Nagumo reaction-diffusion model is introduced. The underlying model provides beneficial properties that have clear advantages for developing a navigation framework, e.g., like natural parallelism and fault tolerance to damaged cells (noisy data). Although there are widely used standard path planning approaches using a grid based map representation (e.g., based on standard state space search algorithms like D* or Theta*), the proposed planning framework is based on different principles coming from natural processes. Moreover, the presented results demonstrate the provided paths are competitive and smoother, therefore the proposed approach provides new quality of solution originated from different principles.

The current computational requirements can be considered as high; however, the relation between the RD dynamics and the geometrical information representing the real world results that all decision-logic takes place naturally through the system evolution. Therefore, increasing the complexity of the environment does not propagate similar effect to the computational burden.

Further studies not shown in this paper have confirmed the ability to extend the presented approach to deal with more advanced navigation tasks (e.g., exploration of unknown environment, or multi-robot navigation) in a straightforward way. The algorithm extension to a 3D environment is also trivial, and let us to envisage future applications. These are subjects of our future work in this field.

Acknowledgments

The access to computing and storage facilities provided under the National Grid Infrastructure MetaCentrum, provided under project No. LM2010005 funded by Ministry of Education of Czech Republic is highly appreciated.

References

[1] V. K. Vanag, "Waves and patterns in reaction diffusion systems. belousovzhabotinsky reaction in water-in-oil microemulsions," *Physics-Uspekhi*, vol. 47, no. 9, p. 923, 2004.

[2] V. I. Krinsky, V. N. Biktashev, and I. R. Efimov, "Autowave principles for parallel image processing," *Phys. D*, vol. 49, no. 1-2, pp. 247–253, 1991.

[3] L. Kuhnert, K. I. Aglazde, and V. I. Krinsky, "Image-processing using light-sensitive chemical waves," *Nature*, vol. 337, no. 6204, pp. 244–247, Jan. 1989.

[4] O. Steinbock, P. Kettunen, and K. Showalter, "Engineering of dynamical systems for pattern recognition and information processing," *J. Phys. Chem.*, vol. 100, pp. 18 970–18 975, 1996.

[5] V. Perez-Munuzuri, V. Perez-Villar, and L. Chua, "Autowaves for image processing on a two-dimensional cnn array of excitable nonlinear circuits: flat and wrinkled labyrinths," *IEEE Transactions on Circuits and Systems I: Fundamental Theory and Applications*, vol. 40, no. 3, pp. 174 –181, mar 1993.

[6] O. Steinbock, K. Showalter, and P. Kettunen, "Navigating complex labyrinths - optimal paths from chemical waves," *Science*, vol. 100, pp. 868–871, 1994.

[7] K. Showalter, R. M. Noyes, and H. Turner, "Detailed studies of trigger wave initiation and detection," *Journal of the American Chemical Society*, vol. 101, no. 25, pp. 7463–7469, 1979.

[8] A. Vázquez-Otero and A. P. Muñuzuri, "Navigation algorithm for autonomous devices based on biological waves," in *12th International Workshop on Cellular Nanoscale Networks and Their Applications (CNNA)*, 2010, pp. 1–5.

[9] A. Adamatzky, B. de Lacy Costello, C. Melhuish, and N. Ratcliffe, "Experimental reaction-diffusion chemical processors for robot path planning," *Journal of Intelligent and Robotic Systems*, vol. 37, no. 3, pp. 233–249, 2003.

[10] A. Adamatzky, P. Arena, A. Basile, R. Carmona-Galan, B. Costello, L. Fortuna, M. Frasca, and A. Rodriguez-Vazquez, "Reaction-diffusion navigation robot control: from chemical to vlsi analogic processors," *IEEE Transactions on Circuits and Systems I: Regular Papers*, vol. 51, no. 5, pp. 926–938, may 2004.

[11] C. Trevai, Y. Fukazawa, H. Yuasa, J. Ota, T. Arai, and H. Asama, "Cooperative exploration path planning for mobile robots by reaction-diffusion equation on graph," in *IEEE International Conference on Industrial Technology (ICIT)*, vol. 2, dec. 2002, pp. 1266–1271.

[12] C. Trevai, Y. Fukazawa, J. Ota, H. Yuasa, T. Arai, and H. Asama, "Cooperative exploration of mobile robots using reaction-diffusion equation on a graph," in *IEEE International Conference on Robotics and Automation (ICRA)*, vol. 2, 2003, pp. 2269–2274.

[13] P. Arena, L. Fortuna, M. Frasca, G. Vagliasindi, and A. Basile, "Cnn wave based computation for robot navigation on ace16k," in *Circuits and Systems, 2005. ISCAS 2005. IEEE International Symposium on*, may 2005, pp. 5818 – 5821 Vol. 6.

[14] K. Ito, M. Hiratsuka, T. Aoki, and T. Higuchi, "A shortest path search algorithm using an excitable digital reaction-diffusion system," *IEICE Transactions*, pp. 735–743, 2006.

[15] A. Willms and S. Yang, "Real-time robot path planning via a distance-propagating dynamic system with obstacle clearance," *IEEE Transactions on Systems, Man, and Cybernetics, Part B: Cybernetics*, vol. 38, no. 3, pp. 884 –893, june 2008.

[16] V. Kilic, R. Yeniceri, and M. Yalcin, "A new active wave computing based real time mobile robot navigation algorithm for dynamic environment," in *12th International Workshop on Cellular Nanoscale Networks and Their Applications (CNNA)*, 2010, pp. 1 –6.

[17] V. Kilic and M. E. Yalcin, "An active wave computing based path finding approach for 3-d environment," in *IEEE International Symposium on Circuits and Systems (ISCAS)*, 2011, pp. 2165 –2168.

[18] R. A. Jarvis, "On distance transform based collision-free path planning for robot navigation in known, unknown and time-varying environments," in *Advanced Mobile Robots*, Y. F. Zang, Ed. World Scientific Publishing Co. Pty. Ltd., 1994, pp. 3–31.

[19] P. Beeson, N. Jong, and B. Kuipers, "Towards autonomous topological place detection using the extended voronoi graph," in *IEEE International Conference on Robotics and Automation (ICRA)*, 2005, pp. 4373–4379.

[20] A. P. Muñuzuri and A. Vázquez-Otero, "The cnn solution to the shortest-path-finder problem," in *11th International Workshop On Cellular Neural Networks and Their Applications*, 2008, pp. 248–251.

[21] J. D. Murray, *Mathematical biology, III edition*. Berlin Springer-Verlag, 2002.

[22] R. FitzHugh, "Impulses and physiological states in theoretical models of nerve membrane," *Biophys. J.*, vol. 1, pp. 445–466, 1961.

[23] J. Chudoba, R. Mázl, and L. Přeučil, "A Control System for Multi-Robotic Communities," in *ETFA 2006 Proceedings*. Piscataway: IEEE, 2006, pp. 827–832.